

# Electrical activity of the PtH<sub>2</sub> complex in silicon: High-resolution Laplace deep-level transient spectroscopy and uniaxial-stress technique

Vi. Kolkovsky,<sup>1</sup> O. Andersen,<sup>2,3</sup> L. Dobaczewski,<sup>1,\*</sup> A. R. Peaker,<sup>2</sup> and K. Bonde Nielsen<sup>4</sup>

<sup>1</sup>*Institute of Physics, Polish Academy of Sciences, al. Lotników 32/46, 02-668 Warsaw, Poland*

<sup>2</sup>*Centre for Electronic Materials, Devices and Nanostructures, University of Manchester, Manchester, United Kingdom*

<sup>3</sup>*Topsil Semiconductor Materials A/S, Frederikssund, Denmark*

<sup>4</sup>*Institute of Physics and Astronomy, University of Aarhus, Aarhus, Denmark*

(Received 3 March 2006; published 26 May 2006)

High-resolution Laplace deep-level spectroscopy combined with the uniaxial stress technique has been used to study stress-energy piezospectroscopic tensor components of the platinum-dihydrogen complex in silicon. The effect of stress on the defect has been observed either as the stress-induced Laplace deep-level transient spectroscopy peak splitting (which is interpreted as an effect of stress on the defect ionization process) or as a stress-induced defect alignment. The latter has been observed for both defect charge states, i.e., singly and doubly negative. The kinetics of the alignment process allowed us to conclude that the energy barrier separating equivalent defect configurations is 1 eV, which means that the complex does not reorient below the room temperature. The character of the lattice relaxation derived from the piezospectroscopic characteristics of the complex suggests that in PtH<sub>2</sub> the hydrogen atoms are not directly bonded to platinum.

DOI: [10.1103/PhysRevB.73.195209](https://doi.org/10.1103/PhysRevB.73.195209)

PACS number(s): 71.55.Cn, 61.72.Ji, 68.55.Ln

## I. INTRODUCTION

Platinum-related deep centers in silicon are widely used to control the minority-carrier lifetime in fast-switching semiconductor devices. On the other hand, it has been observed in many cases that unintentionally introduced hydrogen interacts with transition metal (TM) impurities leading to either their passivation or the formation of new electrically active TM complexes.<sup>1–7</sup> The effect of hydrogen on the electrical properties of platinum has been a point of interest for a long time.<sup>2,8–10</sup> Hydrogen atoms interact with platinum and form new complexes with a different electronic structure. This shifts the platinum electronic levels and could be a reason for a dramatic change in semiconductor device characteristics. The existence of PtH<sub>x</sub> (where  $x=1–3$ ) complexes have been detected by electronic paramagnetic resonance (EPR) (Refs. 1 and 2) and local vibrational mode absorption (LVM)<sup>10</sup> in both *n*- and *p*-type silicon. The platinum-dihydrogen complex (PtH<sub>2</sub>) is of particular interest from the point of view of application of platinum for minority-carrier lifetime reduction in power devices (in order to increase the switching speed) because among all platinum-hydrogen complexes it has the shallowest electronic level. This makes the platinum-dihydrogen center an effective carrier recombination center, but as the electronic level is well away from the midgap position the carrier generation via this defect is less effective and hence the device leakage is reduced.

In spite of a number of different studies by both theoretical and experimental groups<sup>1,9,11–14</sup> there are some uncertainties relating to the PtH<sub>2</sub> structure. It is well known that it possesses  $C_{2v}$  symmetry, which is the result of a static Jahn-Teller distortion combining tetragonal and trigonal components analogous with the isolated negatively charged vacancy. However, the position of hydrogen atoms in platinum-hydrogen complexes is disputed. Uftring *et al.*<sup>9</sup> showed from EPR hyperfine tensor that the Pt-H distance is about 4.2 Å

and this value is remarkably close to the expected Pt-H distance for the vacancylike model with the hydrogen atoms pointing away from the platinum. This is about 4.05 Å (2.35 Å is the Si-Si nearest distance and 1.7 Å is the typical back-bond Si-H distance). Similar results have been also obtained by Huy and Ammerlaan<sup>1</sup> from the measured hyperfine tensor of an acceptorlike PtH<sub>2</sub> defect. These results have been supported by the calculations of Jones *et al.*<sup>12</sup> who predicted that the hydrogen atoms in the PtH<sub>2</sub> complex are bonded to two Si atoms neighboring the substitutional Pt in a way that is similar to the NiH<sub>2</sub> complex. However, Hourahine *et al.*<sup>13</sup> calculated that structures with hydrogen directly attached to platinum are energetically favorable over the ones suggested by Jones *et al.* Experimental work on the PtH<sub>2</sub> complex has been continued by Kamiura *et al.*<sup>14</sup> who studied its reorientation kinetics using a deep-level transient spectroscopic (DLTS) technique combined with uniaxial stress. He has found that the reorientation process starts at temperatures close to 80 K. The relatively low temperature for reorientation may suggest that the model with two hydrogen atoms directly bonded to the platinum atom is a plausible case, as has been suggested by Hourahine *et al.* from theoretical considerations.

The EPR technique can only provide structural information for the platinum-hydrogen complex in its paramagnetic states. Similar information for the defect can be obtained from LVM but only for its optically active modes. In both cases it is not straightforward to manipulate with the charge state of the complex, as to do this necessitates varying the Fermi level via changes in the doping level. By using the DLTS technique combined with uniaxial stress, it is possible to observe the effect of stress on the defect stability and the electronic properties in different charge states. Additionally, the application of high-resolution Laplace DLTS (Ref. 15) with the stress technique provides complementary structural information obtained from the observation of the effect of

stress on the defect electronic level, as we have shown in previous work.<sup>11</sup> In this study we present a comprehensive investigation of the effect of stress on the double acceptor electronic state of the platinum-dihydrogen complex. These results allowed us to perform a piezospectroscopic analysis of both charge states of PtH<sub>2</sub> (paramagnetic and diamagnetic) and to postulate the character of the defect relaxation for the complex in these charge states. From the kinetics of the reorientation process, the reorientation barrier of the PtH<sub>2</sub> complex has been estimated to be about 1 eV by analyzing the stress-induced alignment effect

## II. EXPERIMENTAL PROCEDURE

The samples for this study have been prepared from (100)-oriented phosphorous doped float-zone grown silicon with a resistivity of 21–23 Ω cm. The samples were cut into 7 × 2 × 1 mm bars with the long dimension parallel to one of the major crystallographic directions ⟨100⟩, ⟨110⟩, or ⟨111⟩. A thin platinum layer has been evaporated onto one side of a silicon wafer and diffused in at ~820 °C for 2 h in a nitrogen atmosphere. The samples have been etched for 2 min in a CP4A solution in order to introduce hydrogen and eliminate the high surface concentration of platinum resulting from the U-shape of the in-diffused metal. Additional hydrogen has been introduced during a 30 min soak in a solution of nitric (70%) and hydrofluoric (48%) acids in a 10:1 ratio. The Schottky diodes have been formed by vacuum evaporation of gold on the polished and etched side of the bar. An eutectic InGa alloy has been rubbed onto the back side of the samples to fabricate an ohmic contact. A series of test samples made on randomly oriented pieces of the same wafers according to the procedure described has also been produced for calibration of the platinum and hydrogen diffusion process.

## III. RESULTS AND DISCUSSION

The above sample processing procedure leads to appearance of the PtH<sub>2</sub> complex with energy level, which has been observed in conventional DLTS spectra for a rate window of 20 s<sup>-1</sup> at about 90 K.<sup>11</sup> This energy level of the complex has been shown to be a double acceptor state (–/–) based on detailed studies of its emission and capture behavior.<sup>16</sup> Additionally, the same conclusion has been reached earlier from the EPR measurements where an unoccupied state of PtH<sub>2</sub> was observed as a paramagnetic negative charge state in *n*-type silicon.<sup>9</sup> Using high-resolution Laplace DLTS combined with uniaxial stress, we confirmed that the structure of this defect is of the orthorhombic-I *C*<sub>2v</sub> symmetry, as has been established previously by the EPR technique.<sup>6,9</sup> Figure 1 shows the 90 K Laplace DLTS spectra of PtH<sub>2</sub> (–/–) obtained at zero stress and also under uniaxial stress along the three major crystallographic directions. For each stress direction, the zero-stress peak splits into two well-resolved components. The amplitudes of the split lines sum up to the amplitude of the zero-stress peak. The amplitude ratios of the individual peaks in Fig. 1 agree to within 10% with the ratios expected for a splitting pattern expected for an

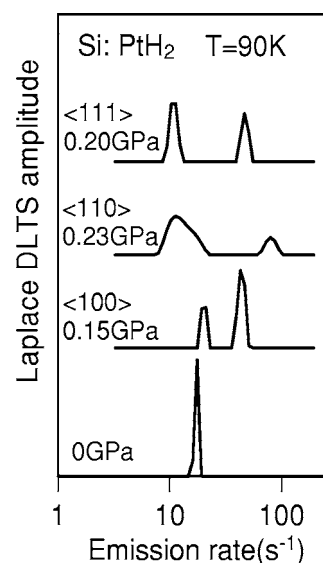


FIG. 1. Laplace DLTS spectra of PtH<sub>2</sub> obtained for stress applied along the three major crystallographic directions, ⟨100⟩, ⟨110⟩ and ⟨111⟩. The splitting pattern confirms the orthorhombic-I symmetry of the PtH<sub>2</sub> complex.

orthorhombic-I center (see, e.g., Ref. 17 for more details), i.e., 2:4 for the ⟨100⟩ stress direction, (1:4):1 for the ⟨110⟩ stress direction (note a broadened larger peak, which could be a result of the unresolved 1:4 splitting), and 3:3 for the ⟨111⟩ stress direction. Table I contains abbreviations of the nonequivalent configurations of PtH<sub>2</sub> in a silicon crystal stressed along major crystallographic directions. The main crystallographic axes are described as shown in Fig. 2. The details of the PtH<sub>2</sub> model will be discussed in the following parts of this work.

In order to obtain more detailed information about the defect lattice relaxation process and structural information concerning the reorientation barriers and, in consequence, the position of the hydrogen atom in the PtH<sub>2</sub> center, two types of experiments have been performed. Firstly, the influence of uniaxial stress on the ionization process of the double acceptor state: PtH<sub>2</sub><sup>–</sup> → PtH<sub>2</sub><sup>–</sup> + e<sub>c</sub><sup>–</sup> has been studied for the different stress directions. Secondly, the so-called alignment process has been investigated, which provides detailed information on the piezospectroscopic tensor for individual charge states.

TABLE I. Abbreviations for the nonequivalent configurations of an orthorhombic defect center in a cubic crystal stressed along three major crystallographic directions. See Fig. 2.

Configuration	Stress direction
1A	[100], [010]
1B	[001]
2A	[110]
2B	[101], [ $\bar{1}$ 01], [011], [0 $\bar{1}$ 1]
2C	[ $\bar{1}$ 10]
3A	[111], [ $\bar{1}$ 11]
3B	[ $\bar{1}$ 11], [1 $\bar{1}$ 1]

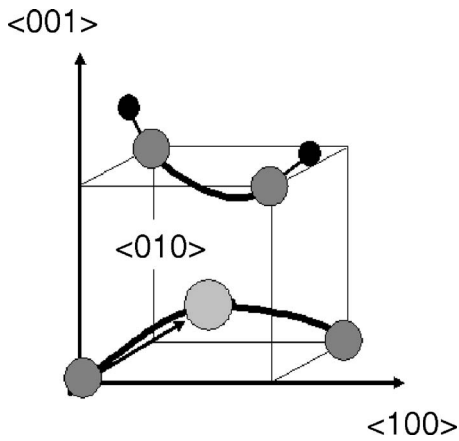


FIG. 2. The vacancylike model of PtH<sub>2</sub> complex where Pt atom (light gray color) occupies an off-center site toward two of four silicon atoms (gray color) and two hydrogen atoms (black), terminating the remaining Si bonds, pointing away of the Pt atom.

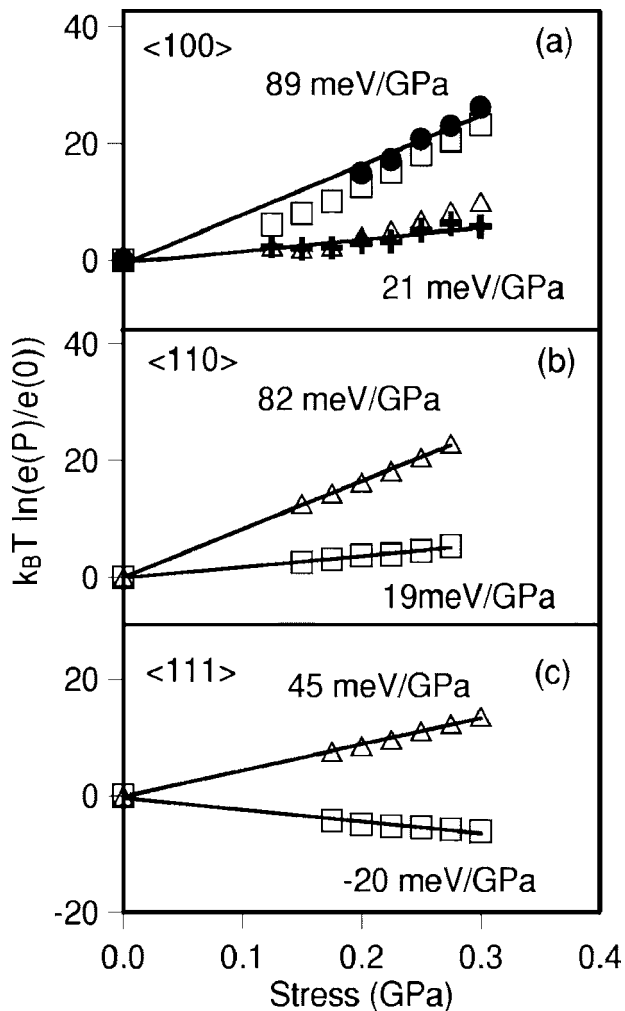


FIG. 3. Laplace DLTS peak shifts versus applied stress along the (a)  $\langle 100 \rangle$ , (b)  $\langle 110 \rangle$ , and (c)  $\langle 111 \rangle$  directions. The full symbols are the values where in formula (1) the stress dependence of the capture cross section on the stress along the  $\langle 100 \rangle$  direction (Fig. 4) has been included (see text for details).

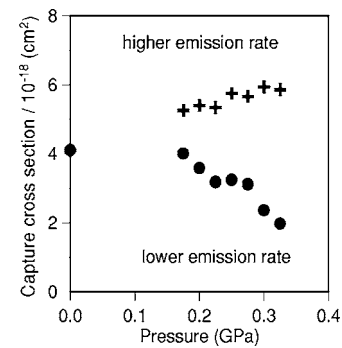


FIG. 4. The PtH<sub>2</sub> capture cross-section pressure dependence (stress-split peaks with smaller and higher emission rates) at  $T=90$  K.

Figure 3 shows the Laplace DLTS split peak shifts versus applied stress  $P$  along the  $\langle 100 \rangle$ ,  $\langle 110 \rangle$ , and  $\langle 111 \rangle$  directions for the different nonequivalent configurations of PtH<sub>2</sub>. The emission rates ( $e_n$ ) of split peaks have been obtained at a number of stress values at 90 K and transformed into energy scale using the well-known equation for carrier emission rate,

$$E(P) = -k_B T \times \ln[Ae_n(P, T)/\sigma_n(P, T)], \quad (1)$$

where  $T$  and  $P$  are the measurement temperature and stress, respectively,  $\sigma_n$  is the capture cross section,  $k_B$  is the Boltzmann constant, and  $A$  is a stress-independent constant. In the first instance, the conversion from the emission rate to an energy scale has been performed using formula (1) assuming that there is no stress dependence of the capture cross section. As a result of this conversion procedure, it is seen that fitted lines of the energy of both the higher and lower emission rate peaks, which have been obtained from regression analysis for  $\langle 110 \rangle$  and  $\langle 111 \rangle$  stress directions, follow a linear dependence and converge at the  $P=0$  point. This behavior is expected from piezospectroscopic theory for the case where the energies of the defect are linearly dependent on the stress. The following stress coefficients for ionization process for all nonequivalent orientations were obtained:  $\alpha_{2B} = \alpha_{2C} = 19$  meV/GPa,  $\alpha_{2A} = 82$  meV/GPa,  $\alpha_{3B} = -20$  meV/GPa, and  $\alpha_{3A} = 44$  meV/GPa.

For the  $\langle 100 \rangle$  orientation, neither the high- nor the low-frequency lines converge at  $P=0$ . Moreover, for the smaller emission rate peak, a clear bowing effect has been observed and reproduced for numerous samples [see open symbols in Fig. 3(a)]. The bowing effect for the smaller emission rate peak suggests that the apparent capture cross section is not independent of the applied stress, as it is for the case of other orientations where a clear linear dependence on stress is observed. In order to explore this effect, a direct measurement of the capture process for both high- and low-frequency lines have been performed for all sample orientations. Figure 4 shows the dependence of the capture cross sections of the split lines on stress applied along the  $\langle 100 \rangle$  direction. For the lower frequency branch, the capture cross section decreases (by about a factor of 2) while for the higher frequency branch it only increases slightly (by about 40%) over the whole range of stresses. No stress dependence has been ob-

served for either of the components of the split peaks for stress applied in the  $\langle 110 \rangle$  and  $\langle 111 \rangle$  orientations.

Taking into account the stress dependence of the capture cross sections for both the smaller and higher emission rates, the open symbols in Fig. 3(a) (for the  $\langle 100 \rangle$  orientation) have been recalculated according to formula (1). As seen in Fig. 3(a) (closed symbols), the bowing effect substantially decreases after this correction. The linear fitting including the zero point gives a better approximation to the stress coefficients of the Laplace DLTS peaks for the  $\langle 100 \rangle$  stress orientation:  $\alpha_{1A} = 89$  meV/GPa and  $\alpha_{1B} = 21$  meV/GPa.

A similar bowing effect has been already observed by us for the case of the piezospectroscopic analysis of the vacancy-oxygen orthorhombic (VO) complex (the *A* center) in silicon.<sup>17</sup> There is a striking correspondence between that case and the bowing observed for PtH<sub>2</sub>, as both defects are observed in the silicon matrix and the bowing is seen for the same branch of the split peak for the  $\langle 100 \rangle$  sample orientation. In addition, the local symmetry of both defects is orthorhombic-I. There could be two reasons that could cause such a stress-induced decrease of the capture cross section for the *1B* stress orientation (see Table I and Fig. 2). Firstly, because of the similarity between the *A* center and PtH<sub>2</sub> complex cases, it is likely that the explanation of the observed effect is a unique aspect of the *1B* stress orientation for a defect with an orthorhombic symmetry. In the silicon unit cell this particular stress orientation causes the strongest compressive strain along the  $[001]$  direction and also the strongest tensile strain along the  $[110]$  direction. Thus one can expect that for this particular stress direction the defect ionization process is accompanied by some specific local lattice relaxation that in turn invokes the appearance of a capture process energy barrier and so reducing the capture cross section. This could be equivalent to the multiphonon capture process postulated by Henry and Lang for a radial defect relaxation process.<sup>18</sup> On the other hand, the equivalence between these two cases also suggests that wave functions of the electron bound by the defect are similar. More detailed discussion of this relaxation effect can be found in Ref. 17. An alternative explanation is that the stress splitting of the conduction band of silicon is strongest for the  $\langle 100 \rangle$  stress orientation. As a result, the capture process can occur for carriers originating from both subbands. The different stress-induced changes in the capture process for both configurations observed for this stress direction may indicate that, for example, the defect in the *1B* configuration prefers to capture electrons originating from one particular subband of the conduction band rather than from the other one. This means that there are some selection rules for the electron capture process. Summarizing, the first explanation of the observed bowing effect refers to the vibrational part of the wave function of an electron bound by the defect. In the other case, it is suggested that the electronic part of the wave function is responsible for the changes in the capture process. Unfortunately, we do not see any experimental way to distinguish between these hypotheses.

While the influence of the stress on the Laplace DLTS peak structure allows us to conclude how the stress modifies the defect ionization process, the defect alignment experiments demonstrate the stress-induced changes in the defect

total energy. These changes can be observed for both the single and double negative charge state of the defect. If stress is applied at temperatures where the complex reorients and then the sample is cooled quickly to the measurement temperature, the complex takes a preferential direction in respect to the stress. This experimental procedure has been applied for all three orientations of samples investigated and the effect of the alignment has been observed as a change in the peak amplitude ratios in respect to the ones observed for the nonaligned defects.

According to these observations, the PtH<sub>2</sub> complex starts to reorientate at temperatures about 300 K and above. When the sample bias is off (which results in the double negative charge state of PtH<sub>2</sub>), this reorientation temperature needs to be higher than for the bias on conditions, i.e., for the single negative charge state. This is in agreement with the generally observed trend, for example, in the vacancy-oxygen<sup>17</sup> and the vacancy-oxygen-hydrogen<sup>19</sup> complexes, where it has been found that the reorientation barrier increases when there are more electrons captured by a complex. The reorientation barriers of vacancy-related orthorhombic (VO) and pseudo-orthorhombic (VOH) complexes are 0.38 eV and 0.56 eV, respectively. In consequence these defects start to reorientate (in a time scale of minutes) at temperatures around 100 K and 200 K for VO and VOH, respectively. In the PtH<sub>2</sub> complex, no vacancies are involved and so, in principle, it might be expected that the lack of empty volume in the unit cell could make the reorientation process much more difficult. As a result, the reorientation barrier would be expected to be much higher than the one observed in the former two cases. On the other hand, it has been observed already that the divacancy V<sub>2</sub> in silicon starts to reorientate at temperatures above 350 K, and in this case this process is thought to be identical with the long-range diffusion of the complex.<sup>20</sup> The diffusion of the divacancy is governed by a 1.3 eV energy barrier. The similarities in the reorientation temperatures of PtH<sub>2</sub> and V<sub>2</sub> allow us to conclude that the barrier for the case of PtH<sub>2</sub> reorientation would be close to or above 1 eV.

On the other hand, this observed tendency of PtH<sub>2</sub> complex reorientation at quite high temperatures does not agree with the data obtained by Kamiura and coworkers,<sup>14</sup> who have suggested that such complexes should reorient at low temperatures (about 90 K) and have evaluated the activation energy for the hydrogen jump to be equal to about 0.27 eV. They have explained such reorientation processes by the model where the two hydrogen atoms are directly bonded to the platinum atom and two silicon atoms are displaced inward, creating a bond. Then in the frame of this model the platinum-dihydrogen complex needs only a simple rotation of the PtH<sub>2</sub> molecule in the silicon vacancy cage to be reoriented with no bond rearrangement. Such a procedure does not need much energy or space to be realized and thus can be activated at quite low temperatures. However, this model cannot explain the Pt-H distance (about 4.2 Å) concluded from the analysis of a small anisotropy in the hydrogen hyperfine interaction.<sup>9</sup> Moreover, in this model the Pt atom is not bonded to the neighboring Si atoms and thus the PtH<sub>2</sub> molecule should have a high diffusivity. This is similar to the case of the interstitial Fe species in silicon. However, detailed studies of the PtH<sub>x</sub> complexes' diffusion and stability

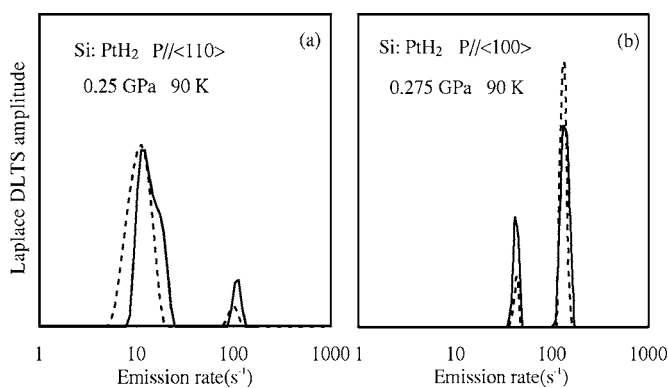


FIG. 5. Laplace DLTS spectra of the double acceptor state of PtH<sub>2</sub>, which have been obtained before (solid line) and after partial alignment (dashed line) when during the alignment the sample was kept in the single and double negative charge state for the cases of the  $\langle 100 \rangle$  and  $\langle 110 \rangle$  direction, respectively.

performed by Sachse *et al.*<sup>21</sup> showed that the PtH<sub>x</sub> diffusion is a result of the hydrogen movement alone and platinum stays in the same lattice position. Finally, the lack of a bond reconstruction process during PtH<sub>2</sub> rotation should result in the fast reorientation of the complex even at temperatures much lower than 90 K. As a result, the symmetry of such complexes observed in the DLTS experiments should change from orthorhombic  $C_{2v}$  (static symmetry of the PtH<sub>2</sub> center) to tetragonal  $C_{4h}$  (dynamic symmetry of a vacancy in silicon). Similar changes in the DLTS defect symmetry for reconfiguring complexes has been observed by us for the case of divacancy<sup>22</sup> in different charge states and for the VOH complex<sup>19</sup> in silicon. For example, based on EPR measurements, Watkins and Corbett<sup>23</sup> showed that for  $V_2^+$  and  $V_2^-$  charge states, the change of symmetry (from trigonal to monoclinic) happens at temperatures slightly above 40 K; thus, this mechanism will be operative at around 120 K, whereas when DLTS measurements for  $V_2^-$  are performed, only trigonal symmetry could be revealed.<sup>22</sup> All the above arguments clearly suggest a more complex character for the reorientation process than a simple rotation of the PtH<sub>2</sub> molecule and show that the vacancylike PtH<sub>2</sub> model is the more plausible case here.<sup>9</sup> According to this model, the Pt atom occupies an off-center site toward two of the four silicon atoms surrounding it. Two hydrogen atoms, terminating the remaining Si bonds, point toward or away from the Pt atom.

As a first stage of the alignment experiments, it has been found that the equilibrium distribution between the non-equivalent orientations has been reached by applying the stress at a relatively high temperature about 300 K for approximately 60 min for the negative charge state of PtH<sub>2</sub> and about 310 K for the double negative one for the same time. Figures 5(a) and 5(b) show Laplace DLTS spectra of the double acceptor state of PtH<sub>2</sub>, which have been obtained before (solid line) and after partial alignment (dashed line); during the alignment the sample was kept in the single and double negative charge state for the case of the  $\langle 100 \rangle$  and  $\langle 110 \rangle$  directions, respectively. For a defect with the orthorhombic symmetry, some defect orientations have equal degeneracies; thus, it is not always obvious which orientation

TABLE II. Values (in meV/GPa) of the alignment stress coefficients in both charge states and the recalculated (see text for details) Laplace DLTS splitting coefficients of the platinum-dihydrogen complex. For the  $\langle 110 \rangle$  stress direction, the peak splitting and defect alignment are only estimated and they are compared with the calculated values obtained from the data for the  $\langle 100 \rangle$  and  $\langle 111 \rangle$  stress directions.

Stress direction	PtH <sub>2</sub> (-)	Laplace DLTS peak splitting	PtH <sub>2</sub> (--)
$\langle 100 \rangle$ measured	-16	68	54
$\langle 111 \rangle$ measured	0	64	67
$\langle 110 \rangle$ measured	0	~60	~130
calculated $\alpha_{2B,2A}$	-7		77
calculated $\alpha_{2C,2A}$	0		101

gains amplitude as a result of the alignment procedure. For the  $\langle 100 \rangle$  direction, there is no such ambiguity, and based on Fig. 5(b), one can see that in the single negative charge state the 1A configuration of PtH<sub>2</sub> is gaining amplitude for negative (compressive) stress. In the case of the  $\langle 111 \rangle$  stress direction, both of the configurations 3A and 3B have the same degeneracy. For the single negative charge state, there is no alignment effect (in contrast to the data presented in Ref. 14); thus, this ambiguity does not create a problem in the data interpretation procedure. However, in the case of the double negative charge state, there are two possible interpretations of the data, i.e., which of the 3A and 3B configurations is gaining the amplitude. Finally, for the  $\langle 110 \rangle$  direction, two configurations, which form a peak at lower emission rates, are not resolved, and thus again one cannot conclude which of them gains in amplitude when the peak at higher emission rates decreases. This is unlike the case of the VO center in silicon where the high-frequency line gains amplitude, which can be identified as one of the nondegenerated configurations 2A or 2C.

Table II gathers the alignment stress coefficients for PtH<sub>2</sub> in both charge states and the Laplace DLTS peak splitting, including recalculated stress coefficients for the  $\langle 100 \rangle$  orientation where the stress dependences of the capture cross sections have been taken into account. Note that all measurements were performed for a negative (compressive) stress; thus, in this table, the opposite values of the obtained stress coefficients are given to comply with a general rule that derivatives for increasing stress should be specified. In general, the effect of stress on the ionization process:  $\text{PtH}_2^{--} \rightarrow \text{PtH}_2^- + e_c^-$  is reflected by the Laplace DLTS peak shift; thus, the peak splitting shows a difference in the stress-induced changes in the ionization process for both defect configurations. The alignment data show the effect of stress on the ionization process in initial and final states. As a result, the stress coefficients in Table II should sum up in rows, i.e., the ones given in the first two columns should give the values in the third column [similar to the results obtained for the VO defect in Si (Ref. 17)]. Within the experimental error, this is what one observes for the  $\langle 100 \rangle$  and  $\langle 111 \rangle$  stress orientations. The discrepancy in the data obtained for the  $\langle 110 \rangle$  stress direction is larger but this can be a result of the ambi-

TABLE III. Values of the piezospectroscopic tensor components in both charge states assuming that the piezospectroscopic tensor is traceless.

Tensor components (eV)	Laplace DLTS <sup>a</sup>	Theory <sup>b</sup>
$B_1^-$	-1	0
$B_2^-$	0.5	0.7
$B_3^-$	0.5	-0.6
$B_1^{--}$	3.7	1
$B_2^{--}$	6.1	2
$B_3^{--}$	-9.8	-3

<sup>a</sup>This work.

<sup>b</sup>Reference 26.

guity in the peak assignment mentioned above for this particular case of the stress orientation.

Within piezospectroscopic theory<sup>24</sup> the way that a defect with an orthorhombic-I symmetry responds to the stress is described<sup>17,25</sup> by the diagonal piezospectroscopic tensor components  $B_1$ ,  $B_2$ , and  $B_3$  directed along  $[001]$ ,  $[1\bar{1}0]$ , and  $[110]$  directions, respectively (see Fig. 2). It is important to emphasize that a change of the coordinate system to the principal directions helps in the interpretation of the piezospectroscopic parameters associated with the defect, i.e., in establishing the total energy change when the defect is compressed along one of the principal directions. Finally, a positive value of the piezospectroscopic tensor component shows that the compressing stress applied along the corresponding direction lowers the defect energy and means an inward defect relaxation along this direction. Measured values of the alignment stress coefficients are linked to the piezospectroscopic tensor components according to the formulas,<sup>17,25</sup>

$$\alpha_{1B,1A} = \frac{(s_{11} - s_{12})(2B_1 - B_2 - B_3)}{2}, \quad (2)$$

$$\alpha_{3B,3A} = \frac{s_{44}(B_2 - B_3)}{3}, \quad (3)$$

$$\alpha_{2B,2A} = \frac{(s_{11} - s_{12})(2B_1 - B_2 - B_3)}{4} + \frac{s_{44}(B_2 - B_3)}{4}, \quad (4)$$

$$\alpha_{2C,2A} = s_{44} \frac{(B_2 - B_3)}{2}, \quad (5)$$

where the configuration labels are given in Table I. For silicon, the components of the elastic compliance tensor are  $s_{11} = 7.68 \times 10^{-3} \text{ GPa}^{-1}$ ,  $s_{12} = -2.14 \times 10^{-3} \text{ GPa}^{-1}$ , and  $s_{44} = 12.6 \times 10^{-3} \text{ GPa}^{-1}$ . Usually, in the stress-data analysis, one assumes that the piezospectroscopic tensor is traceless  $B_1 + B_2 + B_3 = 0$ , i.e., the stress does not change the defect volume.

As one can see, the alignment data for the  $\langle 100 \rangle$  and  $\langle 111 \rangle$  stress directions together with the traceless feature of the tensor are enough to obtain all  $B$ 's for both charge states of

the defect. The values of the  $B$  tensor for the single negative charge state from the data given in Table II and Eqs. (2) and (3) are presented in Table III. These values were used in Eqs. (4) and (5) to obtain the alignment  $\alpha_{2B,2A}$  and  $\alpha_{2C,2A}$  stress coefficients for the  $\langle 110 \rangle$  sample orientation. The calculated values (given in the last two rows of the second column in Table II) are small and fully agree with the lack of an alignment effect for this charge state and sample orientation. The same alignment data analysis for the double negative charge state of the defect has been performed, keeping in mind the peak assignment ambiguity, i.e., which of the configurations (3A or 3B) is represented by the high-emission rate peak in the top spectrum in Fig. 1. If one assumes that this configuration is 3A, then the values of the piezospectroscopic tensor for the double negative charge state can be obtained (Table III). In this case the configuration corresponding to the high-emission rate peak for the  $\langle 110 \rangle$  sample orientation is 2A. In the opposite case (the configuration 3B corresponds to the high-emission rate peak in Fig. 1), the values for  $B_2^{--}$  and  $B_3^{--}$  have to be interchanged and the small line in the  $\langle 110 \rangle$  case is the 2C configuration. However, this alternative analysis does not bring any new qualitative knowledge about the complex.

It has been observed that  $\text{PtH}_2$  in the double negative charge state clearly aligns when stressed along the  $\langle 110 \rangle$  direction. Due to the fact that in this case three energy levels take part in the process, it has to be described by two stress coefficients. The same remark also applies to the splitting effect observed for this sample. As one cannot obtain as many stress coefficients from reliable fitting procedures, the data for  $\langle 110 \rangle$  has been fitted assuming that only 2A and 2B participate in the splitting and alignment for  $\text{PtH}_2^{--}$ . These approximate values are given in Table II. On the other hand, the alignment data obtained for the double negative charge state of the complex for the  $\langle 100 \rangle$  and  $\langle 111 \rangle$  stress orientations enable calculations to be made according to Eqs. (4) and (5) of the two stress coefficients for the  $\langle 110 \rangle$  orientation, which are impossible to obtain directly from the experimental data. These numbers are also presented in Table II. As one can see, both of them are smaller than the value obtained from an approximate two-level analysis of the data. Employing proper formulas for the alignment effect in a three-level system and summing up two unresolved amplitudes of the 2B and 2C configurations, we can reproduce the tendency in the alignment experiment; however, the individual values are, as one could expect, systematically underestimated. The Laplace DLTS peak splitting is a little smaller than the differences between the calculated stress coefficients. However, keeping in mind the rather large experimental uncertainty in this case and that for the  $\langle 110 \rangle$  stress direction both the splitting and alignment in the double negative charge state provide too little information for a comprehensive data analysis procedure, one can state that this agreement is satisfactory.

The values of the piezospectroscopic tensor components obtained from the experimental procedure described above are compared with the ones calculated by Hourahine *et al.*,<sup>26</sup> assuming the same defect structure (see Table III). For the single negative charge state of the complex, the experimental values are small, i.e., much smaller than the ones which we have obtained for the cases of  $\text{V}_2$ ,<sup>22</sup>  $\text{VO}$ ,<sup>23</sup>  $\text{VOH}$ ,<sup>19</sup> and  $\text{CH}$

(Ref. 27) complexes in silicon. On the other hand, similar small values have been found from theoretical modeling procedures, which indicate a good agreement between the experiment and theory. However, it is difficult in this case to refer to particular values of the  $B$  tensor components, as the values themselves and the differences between them are within the experimental error and the calculation accuracy. For the double negative charge state of the complex, the experimental and theoretical values are larger and despite some discrepancies between them one can identify agreement on key issues: the signs of the corresponding values of the  $B$  tensor are the same and the ratios between experimental and theoretical values are maintained. Thus, despite the experimental values for PtH<sub>2</sub><sup>2-</sup> are approximately three times larger, one can conclude that there is some agreement between the experiment and theory in this case as well.

The most important conclusion concerning the microscopic model of PtH<sub>2</sub> comes from the analysis of the piezospectroscopic tensor components for the double negative charge state. Table III shows that the  $B_2$ <sup>-</sup> and  $B_3$ <sup>-</sup> components have opposite signs. A general rule is that the negative value of some component means an outward defect relaxation along the eigenvector referring to that particular component. As a result, following the structure depicted in Fig. 2, the relaxation along the hydrogen plane, i.e., [110] is outward, while along the platinum plane it is inward. This is exactly what one would expect from the microscopic picture of the defect. When platinum is passivated by two hydrogen atoms, they break the Si-Si bond along the 110 direction and saturate two silicon dangling bonds. Consequently, as this Si-Si bond is no longer keeping the unit cell along this particular direction, this should result in the outward defect relaxation. In contrast to this case, for the VO complex in silicon, the defect symmetry is the same and the Si-Si is not broken; thus, both piezospectroscopic tensor components have *the same* positive sign. See Ref. 17 for more details. Finally, based on this observation, one can rule out the PtH<sub>2</sub>

model where two hydrogen atoms are directly attached to platinum as in this case, because similarly to VO, one can expect that  $B_2$  and  $B_3$  should have the same sign.

#### IV. CONCLUSIONS

In summary, we have demonstrated that a use of the Laplace DLTS combined with the uniaxial stress technique is an efficient technique that allows investigating in detail the structure and electrical properties of both diamagnetic and paramagnetic states of the platinum-dihydrogen complex. The studies of the complex reorientation and alignment make it possible to conclude that this complex does not reconfigure at temperatures below room temperature for bias on and bias off conditions, i.e., in the single and double negative charge state, and that the reconfiguration barrier for nonequivalent configurations is about 1 eV. This is in agreement with the defect model where both hydrogen atoms are attached to silicon atoms and the reorientation of such defect needs to rearrange many bonds and, as a result, needs a lot of energy. Our detailed piezospectroscopic defect analysis has provided us with a complete and comprehensive picture of the defect, which allows us to determine the type and direction of the lattice relaxation and so confirm the microscopic picture of the defect.

#### ACKNOWLEDGMENTS

Discussions with B. Hourahine, R. Jones, and V. P. Markevich are acknowledged. This work has been financially supported in Poland in part by the Ministry of Scientific Research and Information Technology Grant No. 4T11B02123 in the United Kingdom by the Engineering and Science Research Council and the Royal Academy of Engineering, and in Denmark by the Danish National Research Foundation through the Aarhus Center for Atomic Physics (ACAP).

\*Corresponding author. Email address: dobacz@ifpan.edu.pl

<sup>1</sup>P. T. Huy and C. A. J. Ammerlaan, *Physica B* **302&303**, 233 (2001); **308-310**, 408 (2001).

<sup>2</sup>T. Mchedlidze, N. Fukta, and M. Suezawa, *Jpn. J. Appl. Phys., Part 1* **41**, L609 (2002); **41**, L967 (2002).

<sup>3</sup>J. Weber, S. Knack, and J.-U. Sachse, *Physica B* **273&274**, 429 (1999).

<sup>4</sup>O. V. Feklisova, A. L. Parakhonsky, E. B. Yakimov, and J. Weber, *Mater. Sci. Eng., B* **71**, 268 (2000).

<sup>5</sup>E. Ö. Sveinbjörnsson and O. Engström, *Phys. Rev. B* **52**, 4884 (1995).

<sup>6</sup>P. M. Williams, G. D. Watkins, S. Uftring, and M. Stavola, *Phys. Rev. Lett.* **70**, 3816 (1993).

<sup>7</sup>M. J. Evans, M. Stavola, M. G. Weinstein, and S. J. Uftring, *Mater. Sci. Eng., B* **58**, 118 (1999).

<sup>8</sup>J.-U. Sachse, J. Weber, and E. Ö. Sveinbjörnsson, *Phys. Rev. B* **60**, 1474 (1999).

<sup>9</sup>S. J. Uftring, M. Stavola, P. M. Williams, and G. D. Watkins, *Phys. Rev. B* **51**, 9612 (1995).

<sup>10</sup>M. G. Weinstein, M. Stavola, K. L. Stavola, S. J. Uftring, J. Weber, J. -U. Sachse, and H. Lemke, *Phys. Rev. B* **65**, 035206 (2001).

<sup>11</sup>V. Kolkovski, O. Andersen, L. Dobaczewski, A. R. Peaker, and K. Bonde Nielsen, *Physica B* **340-342**, 677 (2003).

<sup>12</sup>R. Jones, S. Öberg, J. Goss, P. R. Briddon, and A. Resende, *Phys. Rev. Lett.* **75**, 2734 (1995).

<sup>13</sup>B. Hourahine, R. Jones, S. Öberg, P. R. Briddon, and T. Frauenheim, *Physica B* **340-342**, 668 (2003).

<sup>14</sup>Y. Kamiura, K. Sato, Y. Iwagami, Y. Yamashita, T. Ishiyama, and Y. Tokuda, *Phys. Rev. B* **69**, 045206 (2004).

<sup>15</sup>L. Dobaczewski, P. Kaczor, I. D. Hawkins, and A. R. Peaker, *J. Appl. Phys.* **76**, 194 (1994); L. Dobaczewski, A. R. Peaker, and K. Bonde Nielsen, *ibid.* **96**, 4689 (2004).

<sup>16</sup>J.-U. Sachse, E. Ö. Sveinbjörnsson, N. Yarykin, and J. Weber, *Mater. Sci. Eng., B* **58**, 134 (1999).

<sup>17</sup>L. Dobaczewski, O. Andersen, L. Rubaldo, K. Gościński, V. P. Markevich, A. R. Peaker, and K. Bonde Nielsen, *Phys. Rev. B* **67**, 195204 (2003).

- <sup>18</sup>C. H. Henry and D. V. Lang, *Phys. Rev. B* **5**, 989 (1977).
- <sup>19</sup>J. Coutinho, O. Andersen, L. Dobaczewski, K. Bonde Nielsen, A. R. Peaker, R. Jones, S. Öberg, and P. R. Briddon, *Phys. Rev. B* **68**, 184106 (2003).
- <sup>20</sup>L. Dobaczewski, K. Bonde Nielsen, O. Andersen, L. Rubaldo, K. Gościński, and A. R. Peaker, in *Proceedings of the 25th International Conference on the Physics of Semiconductors, Osaka 2000*, edited by N. Miura and T. Ando (Springer Proceedings in Physics, New York, 2001), p. 1427.
- <sup>21</sup>J.-U. Sachse, E. Ö. Sveinbjörnsson, W. Jost, J. Weber, and H. Lemke, *Phys. Rev. B* **55**, 16176 (1997).
- <sup>22</sup>L. Dobaczewski, K. Gościński, Z. R. Żytkiewicz, K. Bonde Nielsen, L. Rubaldo, O. Andersen, and A. R. Peaker, *Phys. Rev. B* **65**, 113203 (2002).
- <sup>23</sup>G. D. Watkins and J. W. Corbett, *Phys. Rev.* **138**, A543 (1965).
- <sup>24</sup>A. A. Kaplyanskii, *Opt. Spectrosc.* **10**, 83 (1961); **16**, 329 (1964).
- <sup>25</sup>G. D. Watkins and J. W. Corbett, *Phys. Rev.* **121**, 1001 (1961).
- <sup>26</sup>B. Hourahine, R. Jones, S. Öberg, P. R. Briddon, and T. Frauenheim (unpublished).
- <sup>27</sup>O. Andersen, A. R. Peaker, L. Dobaczewski, K. Bonde Nielsen, B. Hourahine, R. Jones, P. R. Briddon, and S. Öberg, *Phys. Rev. B* **66**, 235205 (2002).